

## CLUSTER EMISSION UNDER FEMTOSECOND LASER ABLATION OF SILICON

Alexander V. Bulgakov,<sup>1,\*</sup> Igor Ozerov,<sup>2</sup> and Wladimir Marine<sup>2,†</sup><sup>1</sup>*Institute of Thermophysics SB RAS, Prospect Lavrentyev 1, 630090 Novosibirsk, Russia*<sup>2</sup>*GPEC, UMR 6631 CNRS, Faculté des Sciences de Luminy, Case 901, 13288 Marseille Cedex 9, France.*

Rich populations of clusters have been observed after femtosecond laser ablation of bulk silicon in vacuum. Size and velocity distributions of the clusters as well as their charge states have been analyzed by reflectron time-of-flight mass spectrometry. An efficient emission of both neutral silicon clusters  $\text{Si}_n$  (up to  $n = 6$ ) and their cations  $\text{Si}_n^+$  (up to  $n = 10$ ) has been observed. The clusters are formed even at very low laser fluences, below the ablation threshold, and their relative yield increases with fluence. We show the dependencies of the cluster yield as well as the expansion dynamics on both laser wavelength and laser fluence. The mechanisms of the cluster formation are discussed.

*Keywords:* Silicon; Nanoclusters; Femtosecond laser ablation; Coulomb Explosion

The recent development of femtosecond lasers expands the possible applications of laser ablation. However, the fundamental mechanisms of light-material interactions are still poorly understood. A study of the plume composition and its expansion helps in understanding of the fundamental processes involved into the interaction and in the development of new laser applications. Recently, surface modifications under femtosecond laser irradiation of bulk silicon have been analyzed for laser pulse durations from 5 to 400 fs [1]. The pump-and-probe studies show the moment of the plasma initiation and allow one to follow the plume expansion at the very early stages close to the target [2]. The first observation of the silicon plume expansion at larger time scale after the femtosecond ablation by time-of-flight methods was reported in [3], where the authors also mentioned the observation of small nanoclusters. However, very few information is available on the formation of silicon nanoclusters after the ablation by short laser pulses. The dimer desorption under resonant nanosecond excitation has been recently reported in the case of (2x1) reconstructed (100) silicon surface [4]. The use of high energy photons of 6.4 eV (ArF laser) induces very strong desorption and ablation of atomic species and small clusters from both the bulk material and the nanostructured Si surfaces [5]. However, there is no systematical information neither on composition nor on the dynamical properties of the plumes induced by femtosecond irradiation. In this work, we present evidence for the formation of clusters with sizes up to 10 atoms under ultrashort laser ablation of bulk silicon and analyze the dynamics of their expansion.

\*Electronic address: bulgakov@itp.nsc.ru (A.V. Bulgakov)

†Corresponding author:

Phone: +33 4 91 82 91 73

Fax: +33 4 91 82 91 76

Electronic address: marine@crmcn.univ.mrs.fr (W. Marine)

## I. EXPERIMENTAL

The experiments were performed with Si [100] surface under ultrahigh vacuum conditions ( $\sim 10^{-10}$  mbar). The monocrystalline Si target was irradiated at an angle of incidence of  $45^\circ$  using a Ti:sapphire laser system (Mai-Tai coupled with TSA amplifier, Spectra Physics, 80 fs pulse duration, 10 Hz repetition rate, up to 30 mJ energy per pulse) operating at wavelengths of 800, 400, and 266 nm. A part of the laser beam was selected by an aperture to provide a nearly uniform intensity distribution over the irradiated spot. The target was rotated/translated during measurements to avoid considerable cratering. For each wavelength, series of craters at several laser energies were produced on the stationary sample. By measuring the crater areas, the absolute calibration of laser fluence was performed. The laser fluence on the target was varied in the ranges 80–800, 20–200, 5–50 mJ/cm<sup>2</sup> at wavelengths of 800, 400, and 266 nm, respectively.

The abundance distributions of neutral and cationic particles in the laser-induced plume were analyzed by a reflectron time-of-flight mass spectrometer (TOF MS). When ions were studied, the plume was allowed to expand under field-free conditions. While the neutral particles of the plume were analyzed, the ionized species were rejected using a simple plasma suppressor [6]. The latter consisted of a pair of deflection plates placed along the plume axis in front of the ion source of the MS where neutral particles were ionized by impact of 110 eV electrons. At a distance of 11 cm from the target, the ions, either ablated or post-ionized, were sampled parallel to the plume expansion axis by a 500 V repeller pulse after a delay time  $t_d$ , following the laser pulse. All mass spectra were averaged over 300 laser shots.

## II. RESULTS AND DISCUSSION

Efficient emission of both neutral silicon clusters  $\text{Si}_n$  (up to  $n = 6$ ) and their cations  $\text{Si}_n^+$  (up to  $n = 10$ ) have been observed for all investigated wavelengths. Si atoms and  $\text{Si}^+$  ions were the most abundant particles at all laser

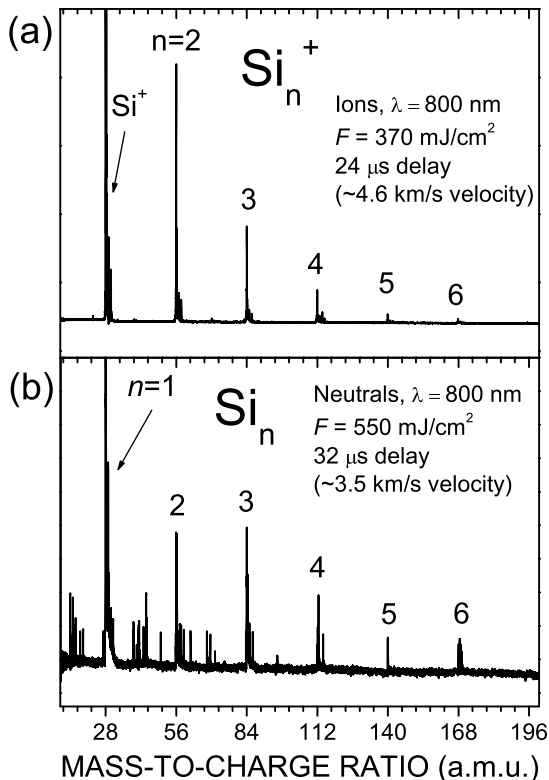


FIG. 1: Mass spectra of cationic (a) and neutral (b) species. The irradiation conditions are indicated in the figure.

fluences. Though, at certain irradiation regimes, the cluster fraction exceeded 10% of that of Si atoms and ions in the ablation plume. Fig. 1 shows typical mass spectra of cationic and neutral plume species, respectively. The spectra were obtained under the irradiation conditions corresponding to the maximum relative yield of the clusters with respect to monatomic particles. The abundance distributions are smooth under these conditions with peak intensities monotonously decreasing with cluster size. As it will be discussed below, the velocity distributions for ionized plume particles are strongly dependent on particle mass. The ion mass spectra are, therefore, different for particles expanding in the faster and the slower parts of the plume. The mass spectrum shown in Fig. 1a was obtained at the time delay corresponding to the maximum yield of  $\text{Si}_2^+$  dimer.

A variation in the time delay  $t_d$  allowed the analysis of particle velocity distributions and the characterization of the temporal evolution of the plume composition. Figure 2 shows typical TOF distributions of  $\text{Si}^+$  ions for different fluences. We have found that the distributions are weakly affected by both laser wavelength and fluence. In all cases, they reach the maximum at  $\sim 9$   $\mu\text{s}$  time delay that corresponds to the ion velocity of around 12 km/s,

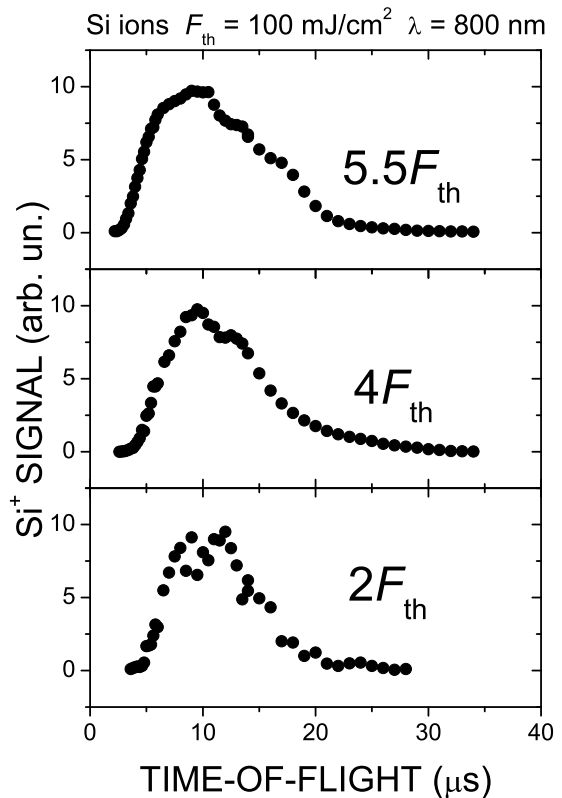


FIG. 2: Typical time-of-flight (TOF) distributions of  $\text{Si}^+$  ions for different fluences. Laser wavelength was 800 nm.  $F_{th} = 100$  mJ/cm<sup>2</sup> is the threshold fluence corresponding to the ion appearance in the plume.

or to a kinetic energy of  $\sim 20$  eV. An increase in laser fluence results only in a broadening of the distributions with a negligible shift towards higher velocities. At the same time, the total number of  $\text{Si}^+$  ions increases strongly with fluence. The ion yield at a given fluence can be evaluated by integrating the TOF distributions in time. To obtain the values proportional to the total number of the plume particles at various fluences, this procedure should be corrected for angular distributions of expanding particles as a function of their velocity (usually fast plume species are more forward directed than slow ones [7, 8]). The angular distributions were not measured in this work, but, since the ion velocity distributions are similar for different conditions (Fig.2), such a correction is not necessary for  $\text{Si}^+$  ions.

Figure 3 shows the yields of plume ions as a function of laser fluence for three laser wavelengths. These dependencies show a steep gradient that is nearly identical for 800 and 400-nm wavelengths. For 266-nm, it is slightly weaker. We note that the total number of detected particles varies by around 6 orders of magnitude in the studied fluence ranges. The threshold fluences,  $F_{th}$ , for ion appearance in the plume, as deduced from MS measure-

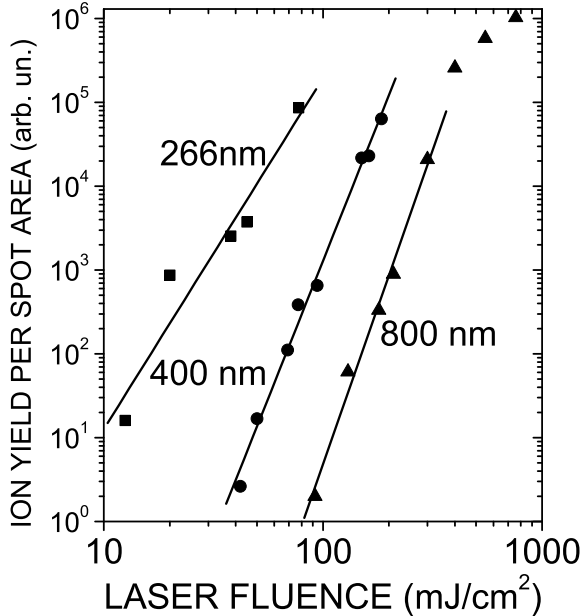


FIG. 3: The ion yield as a function of laser fluence for 800, 400 and 266 nm wavelengths of irradiation.

ments are around 100, 40, and 10 mJ/cm<sup>2</sup> for 800, 400, and 266 nm, respectively. It should be noted that our ion detection system has a high sensitivity to detect a single plume ion. As a result, the obtained values correspond to the *real* thresholds for ion appearance but not to the ion *detection* threshold.

Cluster ions Si<sub>n</sub><sup>+</sup> were observed throughout the laser fluence range studied, even at very low fluences close to the threshold for Si ions (at least for dimers). The clusters are found to be considerably slower than atomic ions. At near-threshold fluences, the TOF distributions for Si<sub>2</sub><sup>+</sup> dimers are maximized at  $t_d \cong 18 \mu\text{s}$  for all wavelengths. The most probable velocity of the dimers is, therefore, approximately two times lower than that of Si<sup>+</sup>. This means that these plume particles have nearly the same momentum under these conditions. However, the Si<sub>3</sub><sup>+</sup> trimers are faster than it would be expected for constant momentum (the TOF distributions are maximized at around 21  $\mu\text{s}$ ).

By integrating the cluster TOF distributions in time, the total number of clusters in the plume as a function of fluence was also evaluated. For low fluences, the total number of the detected dimers increases with fluence and reaches maximum at  $F/F_{th} \cong 2$  for 800 nm and at  $F/F_{th} \cong 4$  for 400 nm. The maximum values of the population ratios Si<sub>2</sub><sup>+</sup>/Si<sup>+</sup> are around 0.18 and 0.22 for 800 and 400 nm respectively. Further increase in fluence results in an abrupt fall of the relative concentration of the dimers. This decrease of the Si<sub>2</sub><sup>+</sup> abundance in the plume is due to both overall decrease of the relative clus-

ter yield at high fluences and to a conversion of Si<sub>2</sub><sup>+</sup> into larger cluster. The performed TOF integration shows the fast increase of the Si<sub>4</sub><sup>+</sup> and Si<sub>6</sub><sup>+</sup> cluster abundance with fluence at  $F > 400 \text{ mJ/cm}^2$ .

In contrast to Si<sup>+</sup> ions, the TOF distributions of clusters strongly depend on the laser fluence. Figure 4 shows the evolution of the TOF distribution for the Si<sub>2</sub><sup>+</sup> dimer at different fluences. These results were obtained for excitation at 800 nm. At very low fluences, below  $\sim 200 \text{ mJ/cm}^2$  ( $\cong 2F_{th}$ ), the distributions are rather narrow, single-peaked, and maximized at  $\sim 18 \mu\text{s}$ . For laser fluences above  $2F_{th}$ , the behavior of Si<sub>2</sub><sup>+</sup> changes dramatically. In the fluence range between  $2F_{th}$  and  $4F_{th}$ , the TOF distributions are still single-peaked but their maxima are significantly shifted towards higher time delays (lower velocities). At  $F = 4F_{th}$ , the maximum is at  $\sim 25 \mu\text{s}$  (the corresponding most probable velocity is  $\sim 4.4 \text{ km/s}$ ). The fast cluster ions are still present in this ablation regime, as can be seen in Fig. 4, but their distribution is masked by slower ions. With further increase in laser fluence the second slower population of Si<sub>2</sub><sup>+</sup> ions with the most probable velocity of around 2.7 km/s appears in the plume. At fluences above  $\sim 5.5F_{th}$ , this slow population becomes dominant. The first faster peak in the distribution (corresponding to the cluster ions detected in the  $(2-4)F_{th}$  fluence range) is still present, well separated from the second peak, and is still maximized at  $\sim 25 \mu\text{s}$ . However, its intensity is much lower than at low fluences. The fast cluster ions (those observed at  $F < 2F_{th}$ ) are not detected anymore.

The fluence dependency of the TOF distributions for larger Si<sub>n</sub><sup>+</sup> clusters ( $n = 3-6$ ) under 800-nm excitation is found to be qualitatively similar to that for Si<sub>2</sub><sup>+</sup>. At a threshold fluence of around 450 mJ/cm<sup>2</sup>, the distributions are transformed from the single-peaked one to the double-peaked with the second (slow) cluster population becoming rapidly dominant with further increase in fluence. The most probable velocity of the second population slightly decreases with cluster size from 2.5 km/s for Si<sub>2</sub><sup>+</sup> to 2 km/s for Si<sub>6</sub><sup>+</sup>. The abundance distribution for this slow cluster population is remarkably different from that for fast clusters (shown in Fig. 1a). The Si<sub>4</sub> and Si<sub>6</sub> cluster ions are more abundant than their odd-numbered neighbors. For larger time delays, the Si<sub>6</sub> cluster becomes dominant particle in the plume.

Based on the obtained results, we can address the fundamental questions on the mechanism of cluster formation. Are the observed clusters formed primarily by their direct ejection from the target or by gas-phase aggregation of ablated atoms? Which process is responsible for such a transformation of the cluster velocity distribution as shown in Fig. 4? The set of the obtained TOF distributions and fluence dependencies provides a clear evidence for cluster formation mechanisms at different irradiation regimes. At very low laser fluence, from ion appearance threshold  $F_{th}$  up to  $\sim 2F_{th}$ , Si<sup>+</sup> and Si<sub>2</sub><sup>+</sup> ions are produced by an impulsive Coulomb explosion (CE) from a charged surface. We argue this by the following:

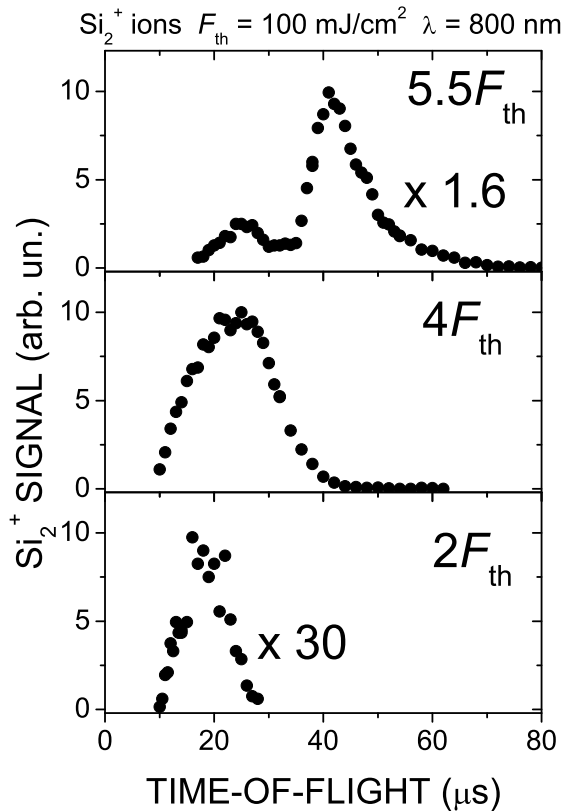


FIG. 4: TOF distributions of  $\text{Si}_2^+$  for irradiation with different fluences at laser wavelength of 800 nm.

(a) The observed momentum scaling for the particles and a very weak dependence of their expansion velocities on laser fluence and wavelength in the low fluence regimes indicates directly the CE mechanism [7]. The repulsive electric field induced in the target by the fs-laser pulse lasts for a short period of time ( $\sim 1$  ps). Both  $\text{Si}^+$  and  $\text{Si}_2^+$  spend roughly the same time in the action range of

this field. The time of electrostatic interaction leading to the ion removal is thus many orders of magnitude shorter than the ion flight time to the mass spectrometer that results in equal momenta for the ejected  $\text{Si}^+$  and  $\text{Si}_2^+$  ions as seen experimentally (Fig.4). We suggest that the electric field under these conditions is strong enough to repulse positive ions from the surface but not so strong to break the bonds of ejected clusters. Note that thermally desorbed particles are characterized by equal kinetic energy rather than momentum [7].

(b) An additional support for the CE is the high velocity of  $\text{Si}_2^+$  ions at low fluences. For fluences beyond  $\sim 2F_{th}$ , the most probable velocity decreases that indicate the appearance of an additional ablation channel. For thermally desorbed particles one would expect the opposite behavior with fluence.

Contrarily, the slower  $\text{Si}_n^+$  clusters (which overshadow the Coulomb explosion ions in the  $2F_{th}-4F_{th}$  fluence range and form the fast cluster population at higher fluences) can be interpreted as "plasma ions", i.e., ions formed in the gas-phase ionized vapor plume. Also, we should take in consideration the direct thermal evaporation of small clusters from the surface (desorption of  $\text{Si}_n$  clusters up to  $n = 6$  was observed from thermally heated Si [9]). The velocities of these "plasma ions" decrease only slightly with cluster size and scale by a law intermediate between constant kinetic energy and constant velocity.

### III. CONCLUSIONS

In conclusion, we present the first analysis of expansion dynamics of monoatomic species and small clusters after femtosecond laser ablation of clean (100) Si surface. While our results unambiguously show the domination of nonthermal mechanism of nanocluster emission at low laser fluence, more studies is needed to be certain about the origin of the ions under all the irradiation conditions.

- 
- [1] J. Bonse, S. Baudach, J. Krüger, W. Kautek, M. Lenzner, Appl. Phys. A **74** (2002) 19.  
 [2] T.Y. Choi, C.P. Grigoropoulos, J. Appl. Phys. **92** (2002) 4918.  
 [3] A. Cavalleri, K. Sokolowski-Tinten, J. Bialkowski, M. Schreiner, D. von der Linde, J. Appl. Phys. **85** (1999) 3301.  
 [4] J. Kanasaki, M. Nakamura, K. Ishikawa, K. Tanimura, Phys. Rev. Lett. **89** (2002) 257601.  
 [5] L. Patrone, I. Ozerov, M. Sentis, W. Marine, J. Phys. IV **11**(2001) Pr7-121. (arXiv: cond-mat/0311336)  
 [6] A.V. Bulgakov, O.F. Bobrenok, V.I. Kosyakov, Chem. Phys. Lett. **320** (2000) 19.  
 [7] R. Stoian, D. Ashkenasi, A. Rosenfeld, E.E.B. Campbell, Phys. Rev. B **62** (2000) 13167.  
 [8] N.M. Bulgakova, A.V. Bulgakov, O.F. Bobrenok, Phys. Rev. E **62**(2000) 5624.  
 [9] H. Tanaka, T. Kanayama, J. Vac. Sci. Technol. B **15** (1997) 1613.